

Quantification of Flow Hydrodynamics in Pulse Thermogravimetric Analysis Systems

A test has been designed and used to compare flow hydrodynamics in different thermogravimetric analysis (TGA) systems used as pulse microreactors. The test involves passing a pulse of injectant over the sample pan containing an adsorbent. Water and zeolite are used in the present case. The technique is easily performed and is insensitive to variations in temperature. A model is developed by which the fraction of gas pulse bypassing the sample pan within the TGA can be obtained. In gas/solid reactions, either catalytic or noncatalytic, the test should prove useful for comparing TGA extent-of-conversion data to similar measurements taken from other reactor configurations, carrier flow rates, and flow geometries.

D. B. Dadyburjor, J. W. Dean
Department of Chemical Engineering
West Virginia University
Morgantown, WV 26506

Due to improvements in microbalance construction, thermogravimetric techniques are being adapted to a growing number of applications. Gravimetric techniques were once considered inappropriate for the study of catalysts, which by definition are supposed to remain unchanged during chemical reactions. During the last decade, however, the availability of advanced surface-sensitive analytical tools has focused interest upon the deactivation of heterogeneous catalysts. The deactivating species may be in the form of feed impurities, as in the case of poisoning, or reaction intermediates, as in the case of coking. Early work with thermogravimetric analysis (TGA) by Massoth (1967) has demonstrated the use of the flow microbalance to develop kinetic data from the continuous oxidation of a coked silica-alumina catalyst. Micropulse techniques have the advantage of allowing one to study initial rates, catalyst deactivation, and other relaxation phenomena. A complete review of micropulse techniques is provided by Choudhary and Doraiswamy (1972). The pulse microreactor combined with TGA may be used for the study of catalyst activity and for comparing catalysts.

In general, not all of the reactants pulsed into the TGA can be expected to contact the catalyst in the sample pan of the TGA. The fraction of the pulsed reactants actually contacting the catalyst could be expected to depend upon the flow hydrodynamics. This may vary from one TGA to the next, particularly if different equipment models are compared, for example, internal oven types vs. external oven types. The flow rate of carrier gas might also influence the hydrodynamics, as might the presence

of constrictors in the flow paths. It is of interest to obtain a comparative value of this fraction. This can be done if a different species can be introduced as a pulse such that any part of it contacting a solid in the sample pan would immediately be adsorbed. Further, the solid should be of similar size, shape, and amount to that used in the reaction experiments, and flow rates of carrier gas and pulse volume should be similar to the corresponding values used during reaction. The temperature should be as low as practicable, to maximize adsorption by the solid on the sample pan.

The present paper describes such a method for calibrating the TGA hydrodynamics. Isothermal gravimetric data are related (as a function of time) to adsorption and desorption phenomena in a model that allows the adsorbed fraction of the initial pulse to be calculated. This fraction is shown to be useful as a direct characteristic of TGA hydrodynamics.

Experimental Method

A diagram of the apparatus, Figure 1, shows the TGA system, which provides for continuous carrier flow and for micropulse injection by means of a syringe and a flexible septum injection port. The TGA microreactor used for this experiment is a Cahn System 113, which features a model 2000 microbalance and an external microprocessor-controlled furnace. By operating the microbalance as a pulse-type microreactor, we can simulate typical industrial riser-tube (hydrocarbon cracking) reaction conditions of 5s contact time and 800 K reaction temperature, virtually free from macroscopic gradients. A constant temperature is accurately maintained and controlled with an external furnace and a thermocouple just below the sample pan.

Correspondence concerning this paper should be addressed to D. B. Dadyburjor.

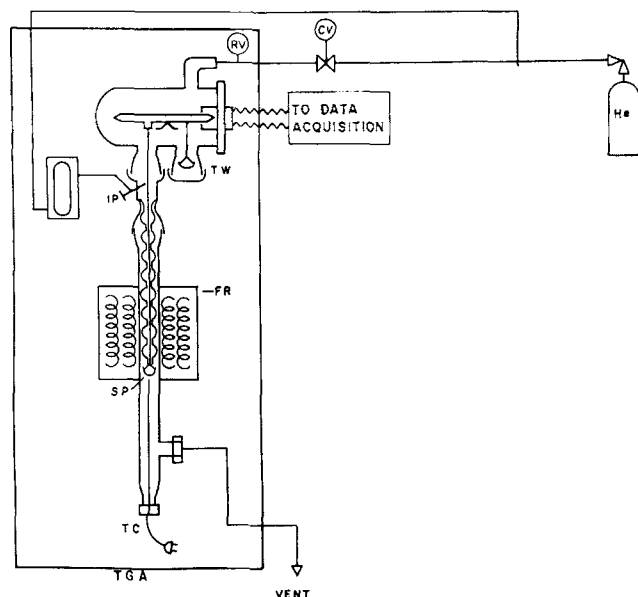


Figure 1. Experimental apparatus.

CV Control valve	RV Relief valve
FR Furnace	SP Sample pan
HE Helium tank	TC Thermocouple
IP Injection port	TW Tare Weight

The weight of a small amount of well-distributed solid catalyst on the platinum sample pan is continuously monitored to measure changes in weight, in this case caused by coke being deposited on the catalyst. The catalyst sample pan is suspended by a thin nichrome wire (inside the Pyrex reactor tube, which is itself inside the TGA furnace) from the weight sensors. A taring system allows weight changes as little as $1.0 \mu\text{g}$ (10^{-9} kg) to be detected even when the sample weight is as high as 50 mg (0.5×10^{-4} kg). Weight changes cause a variable voltage output from the sensor. Analog-to-digital conversion of microbalance output is accomplished by use of an Adalab-PC board installed into one of the expansion slots of an IBM PC computer. The data acquisition and plotting software are provided by Interactive Microware. There is a constant flow of helium through the TGA, both as a carrier gas introduced just above the sample pan, and through a needle valve above the sensors to prevent diffusion of any corrosive gases to the sensors.

Under reaction conditions, the outlet from the TGA (labeled "Vent" in Figure 1) is connected to a sample collection system and a gas chromatograph (GC). The sample collection system allows the TGA to operate at close to atmospheric pressure while the GC operates on-line at 4–5 atm. The collector gathers all of the unconverted reactant that leaves the TGA, without interrupting or altering the steady helium carrier gas flow through the TGA. The outlet from the collector is analyzed by means of a Varian model 3300 GC. The flame ionization detector (FID) on the GC is operated on-line in order to get a complete and rapid analysis.

We are currently using the apparatus to study the catalytic cracking of *n*-hexadecane. One of the components of the cracking catalyst is a rare earth-exchanged Y (REY) zeolite. Zeolites are known to adsorb water strongly at low relative humidities. In addition, it is known that the water adsorption process may be reversed at high temperature without significantly affecting the zeolite. This suggests that zeolite would be a suitable adsorbent,

and water a suitable adsorbate, for the calibration of the hydrodynamics of our TGA system. The carrier gas may be any inert gas that does not adsorb.

We have attempted such an experiment to calibrate the TGA hydrodynamics by pulsing water in a helium stream over solid zeolite material. We have used a REY zeolite (W. R. Grace SMR5-3055) with a surface area of $6.2 \times 10^5 \text{ m}^2/\text{kg}$, preconditioned for several hours by heating the zeolite at 773 K in a flow of helium. This equilibrium procedure establishes ambient humidity conditions of essentially zero and removes all volatile contaminants, so that subsequent adsorption and desorption may be assumed to be due to the water pulse alone.

Figures 2 and 3 are plots of the TGA results when $2 \times 10^{-10} \text{ m}^3$ of water are injected onto $5 \times 10^{-5} \text{ kg}$ of zeolite at 345 K. Figure 2 is obtained by recording one datum point per second for 1,500 s, while Figure 3 consists of five data points per second for the first 30 s of the (same) run, and one point per second for the last 50 s of the run. Note that there are two peaks in Figure 3. The first peak is perhaps due to volume expansion of the liquid pulse when it is vaporized in the flowing stream. The shape of this peak may be affected by the dynamics of the balance. The second, larger, peak is due to adsorption and desorption upon the solid zeolite. (The relationship between the peaks is confirmed by noting the behavior of the microbalance when a similar amount of water is injected over glass beads of low surface area. In the latter case, not shown, only the first peak is noted.)

After 1,500 s, the TGA signals in Figures 2 and 3 level off, but the sample weight does not approach the initial value. Since there was no appreciable baseline change prior to the injection (and since there was no change in the TGA signal before or after the water injection on glass), the change in the signal must be due to "irreversible" adsorption of water on the zeolite at 345 °K. (This adsorption can, in fact, be reversed by heating the zeolite in a stream of He at 773 °K for an hour or less, after which process a second injection of water yields reproducible results compared to Figures 2 and 3.) Changes in the carrier flow rate, and internal reactor alterations that affect the TGA hydrodynamics, cause a change in the curve, but the qualitative features are unchanged.

Analysis

In practice, the material injected does not enter the carrier gas stream as an impulse but as a finite peak, and the width of that peak is further broadened due to axial diffusion between the

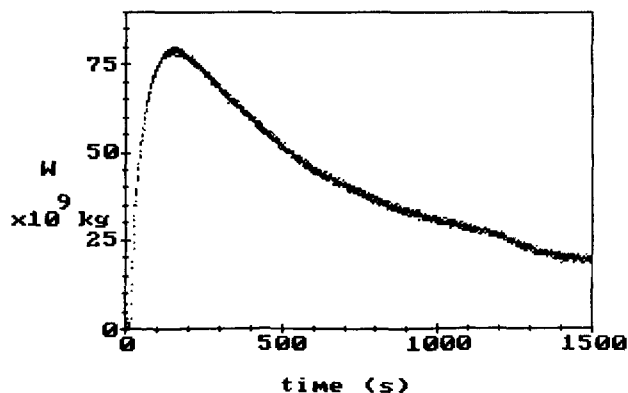


Figure 2. TGA response, 1 datum/s.

$2 \times 10^{-10} \text{ m}^3$ water injected over $5 \times 10^{-5} \text{ kg}$ zeolite at 345 K

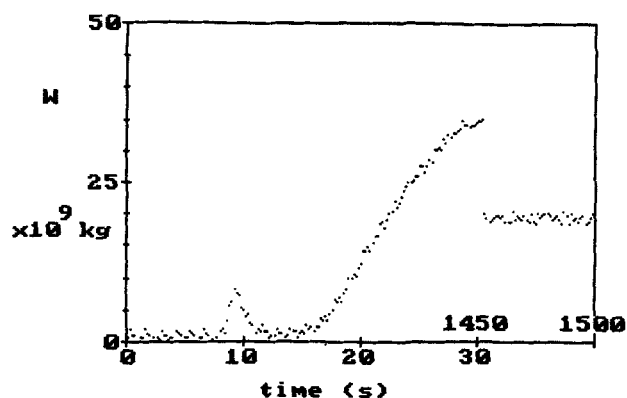


Figure 3. TGA response, 5 data/s for first 30 s, 1 datum/s for last 50 s.

Same run as Figure 2, but note different horizontal scale here and break in scale between $t = 30$ s and $t = 1450$ s

injection point and the adsorbent in the sample pan. Here the injectant may be adsorbed and desorbed, or may bypass the pan and be carried away by the carrier gas. Models for such a process have been advanced, for example to deal with column chromatography (Brown et al., 1978; Zwiebel and Yeo, 1978); however, they are generally too complicated for anything but a numerical solution, and generally yield a number of parameters with a complicated nonlinear fitting process. These parameters are essentially for simulation and predication of results using a given macroreactor, but what is needed in the present work is a single parameter for comparison of different microreactors. Accordingly, a simpler model is used as described below.

The injectant is divided into two parts. A fraction $(1 - f)$ bypasses the sample pan and is removed by the carrier gas. The fraction f is introduced into the gas phase above the sample pan at time t_o that depends upon the carrier gas flow rate and reactor volume. This portion of the injectant is adsorbed and may be desorbed later. The value of f should be independent of temperature and should depend upon the hydrodynamic properties of the system. The parameter f will allow direct comparisons between different systems and flow conditions.

The amount of material present in the gas phase above the sample pan, G , is given by:

$$dG/dt = f \cdot W_o \cdot \delta(t - t_o) - k_a(T) \cdot G \cdot (w_o - w) \quad (1)$$

where the first term on the righthand side is the rate at which the injectant is introduced and the last term is the rate at which the injectant is adsorbed onto the solid. Since our object here is to characterize not the adsorbent but the hydrodynamics, we operate with excess adsorbent present, so that w_o will always be much greater than w . Then:

$$dG/dt = fW_o\delta(t - t_o) - k_a(T)G \quad (2)$$

The amount of injectant actually adsorbed on the pan, w , is given by:

$$dw/dt = k_a(T)G - k_d(T)w_r \quad (3)$$

The first term on the righthand side is the (modified) adsorption rate and the second term is the desorption rate.

Writing w as the sum of "irreversibly" adsorbed material w_i

(unavailable for desorption) and "reversibly" adsorbed material w_r (available for desorption):

$$w = w_i + w_r \quad (4)$$

both w_i and w_r change with time. However, while w_r will increase and then decrease with time, w_i will only increase up to a maximum value and then remain at that value (at least, as long as the temperature is not changed). It is reasonable to assume that the initial adsorption is all of the "irreversible" type until all "irreversible" adsorption sites are occupied. Therefore, there is essentially no desorption of the adsorbate during the short first time it takes w to reach the maximum value of "irreversible" adsorbate, w_a ; see Figure 4. During this initial period, from $t = t_o$ to $t = t_w$, it follows that:

$$w_r = 0 \quad (5a)$$

At times greater than $t = t_w$, it may be assumed that the "irreversible" portion of the adsorbate has reached its maximum value w_a . Then:

$$w_r = w - w_a \quad (5b)$$

The unsteady state material balances given by Eqs. 2, 3, and 5 may be solved with initial conditions:

$$G(0) = 0 \quad (6a)$$

$$w(0) = w(t_o) = 0 \quad (6b)$$

and matching conditions at $t = t_w$, to yield:

$$G = fW_o \cdot U(t - t_o) \cdot \exp[-k_a(t - t_o)] \quad (7a)$$

and

$$w = fW_o(1 - \exp[-k_a[\min(t, t_w) - t_o]]) \cdot U(t - t_o) + [K/(1 - K)]fW_o \exp[-k_a(t - t_o)] \cdot (1 - \exp[-k_a[(1/K) - 1](t_m - t_w)]) \cdot U(t - t_w) \quad (7b)$$

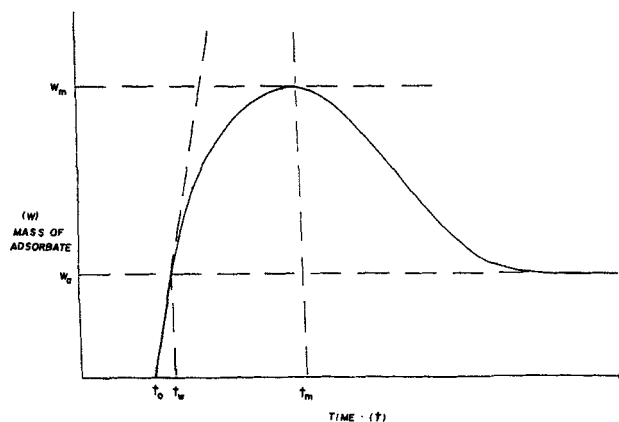


Figure 4. Qualitative plot of w , mass of adsorbate, vs. t , time, derived from Eq. 7b.

where K is a pseudoadsorption equilibrium constant. The form of Eq. 7b is illustrated in Figure 4. As expected, it shows both the maximum in w and the nonzero value of w at large times.

Note that the maximum "irreversible" adsorbate, w_a , can be written as:

$$w_a = fW_o \{1 - \exp[-k_a(t_w - t_o)]\} \quad (8a)$$

the "initial" slope (at $t = t_o$) is given by:

$$(dw/dt)_o = k_a fW_o \quad (8b)$$

the maximum value of w , w_m , can be obtained as:

$$w_m = [K/(1 - K)] fW_o \exp[-k_a(t_m - t_o)] \cdot (1 - \exp[-k_a[(1/K) - 1](t_m - t_w)]) + fW_o \{1 - \exp[-k_a(t_w - t_o)]\} \quad (8c)$$

and the time t_m at which the maximum occurs can be expressed as:

$$t_m - t_w = -\ln(1/K)/[k_a\{1 - (1/K)\}] \quad (8d)$$

Equations 8 allow values of f , k_a , and K to be calculated, but the relations are transcendental. At sufficiently low temperatures, an easier, more direct but more approximate analysis may be used. Under these conditions, K is sufficiently large that:

$$w_m \approx fW_o \{1 - \exp[-k_a(t_m - t_o)]\}$$

Given the additional condition that k_a is large, the further simplification can be made that:

$$w_m \approx fW_o \quad (9a)$$

that is, the value of f can be obtained directly from only the maximum point when adsorption rates are rapid. Under these conditions, the "initial" slope (at t_o) is still given by:

$$(dw/dt)_o = k_a fW_o \quad (9b)$$

and finally the value of K is obtained from:

$$K \approx \exp[k_a(t_m - t_w)] \quad (9c)$$

Results and Discussion

We have injected pulses of 2×10^{-10} m³ of water in a helium flow stream of 8.4×10^{-3} m³/s on 5×10^{-5} kg of zeolite at several temperatures between 313 and 353 K. Values of the maximum point, w_m , vary between 7.8 and 8.0×10^{-8} kg with the exception of one nontypical result of 9.2×10^{-8} kg. Calculations using the approximate method of Eqs. 9 have been performed, and the values obtained are used as initial iterations for the more rigorous calculations of Eqs. 8. Some aspects of these experiments are discussed below.

Equation 2 requires that sufficient adsorbent be used such that the maximum mass of adsorbate capable of being adsorbed, w_o , is much greater than the amount actually adsorbed, w . In order to estimate w_o , the following experiment was performed at ambient conditions: 5.33×10^{-5} kg of an untreated zeolite

sample containing an equilibrium amount of moisture was weighed into the sample pan, heated to 773 K under bone-dry helium, purged, and then cooled by shutting off the furnace heater while maintaining the helium purge. After the sample returned to ambient temperature, it was determined that a loss of 7.4×10^{-6} kg of H₂O had occurred. Compared to this value, the maximum amount of water adsorbed, w_m , is 8×10^{-8} kg, which is two orders of magnitude less than the amount of moisture normally contained at equilibrium conditions. Hence we expect that $w_o \gg w$.

In the operation of a pulse microreactor, the injectant should be introduced as rapidly as possible, to approximate the ideal pulse. In addition, TGA flow characteristics are desired which ensure that axial dispersion in the flow direction is low, so that when the injectant is present above the sample pan, the injectant may be approximated mathematically as a Dirac delta function. The former requirement is well met by use of a hypodermic syringe at the injection site, Figure 1. Calculation of the axial Peclet number at our experimental conditions indicates a large value ($N_{Pe} = 148$), which is consistent with very low axial dispersion. This justifies the use of the initial slope $(dw/dt)_o$ in the model as an indicator of the adsorption rate constant, neglecting nonidealities in pulse shape.

During the experiment, isothermal sample conditions are required since, in addition to the effect of temperature on adsorption, temperature changes are accompanied by changing buoyancy forces. Further, we need to maintain the adsorbent sample at as low a temperature as possible, to maximize the adsorption of water. In our apparatus, the injection point, shown in Figure 1, is heated and insulated to ensure flash-vaporizing the liquid injectant, and the walls of the equipment are also kept hot, to prevent condensation or adsorption of vapor on the inside surface of the TGA. At the lower temperatures near the sample pan, gradients may develop, and these increase the difficulty of measuring the actual sample temperature. Buoyancy forces can normally be tared out, but since the tare pan is outside the furnace, a change in temperature in the furnace causes a deflection in the balance output value. In addition, the furnace is normally operated at high temperatures (up to 1,283 K) and the temperature controller lacks sensitivity at low temperatures.

Slight deviations from isothermal conditions, due to thermocouple response time or other factors, generate a certain amount of temperature-induced baseline drift. Baseline drift may be recorded prior to injection of the water pulse, and a correction may be superimposed upon the TGA response curve. This correction does not influence the maximum point, since the maximum appears very shortly after the introduction of the injectant; at most, the correction may influence the value of the irreversibly adsorbed mass, w_a , which occurs at large values of elapsed time. Due to the above considerations, the furnace is set above ambient temperature conditions; but data taken at the lower temperatures (<323 K) appear to exhibit more fluctuations and less reproducibility.

The baseline results are shown in Table 1. For our apparatus, configured as in Figure 1, the value of f is calculated to be 0.405 ± 0.010 , disregarding the data at 323 K. The pulse technique is not recommended as a procedure for calculating the adsorption equilibrium constant, K . Its estimation from the experimental data is much more subject to error than f . Further, heats of adsorption at low coverages, such as we have here, are much greater than values at higher coverages.

Table 1. Results Before Installation of Diffusion Eliminator at Various Furnace Temperatures

Furnace Temp. K	$K = k_a/k_d$		$k_a, \text{s} \times 10^{-2}$		f	
	Approx.	Exact	Approx.	Exact	Approx.	Exact
345	97.7	74.7	3.49	3.33	0.396	0.415
332	201.3	182.2	3.90	3.83	0.398	0.405
323	165.5	139.9	3.56	3.47	0.388	0.398
323	410.0	374.9	3.55	3.51	0.464	0.470

In the process of optimizing our equipment, we have changed the hydrodynamics of the TGA by installing a diffusion eliminator between the balance container and the injector. The diffusion eliminator, not shown in Figure 1, is in the form of a thin disk with a small hole for the hangdown wire that suspends the sample pan from the balance. The small hole increases the velocity of the container purge at the injection point and makes back-diffusion more difficult. There is no change in the average flow rate at the sample pan, but the flow pattern may change, and this would be expected to change the value of f . This was checked by repeating the series of injections after this equipment revision, with all other conditions maintained the same as before. The results of these experiments are shown in Table 2. If the lower temperature runs are neglected, as in Table 1, the analysis indicates an f value of 0.444 ± 0.010 , appreciably greater than that of Table 1. The TGA hydrodynamics are altered by installation of the diffusion preventer, and this is quantified by the change in the value of f .

The TGA hydrodynamics are also expected to change when we change the carrier flow rate. The overall carrier flow rate is increased from 8.4×10^{-3} to $10.8 \times 10^{-3} \text{ m}^3/\text{s}$, and the first row of Table 3 shows the results from a $2 \times 10^{-10} \text{ m}^3$ water pulse on $5.37 \times 10^{-5} \text{ kg}$ of zeolite at 323 K under the increased flow conditions (and with the diffusion eliminator installed). Unfortunately, the experiment was performed at the low furnace temperature, which we subsequently determined to be of less reliable accuracy. This uncertainty notwithstanding, the value of f as indicated by Table 3 appears to be slightly higher (0.464) at the slightly higher purge rate. These values correspond to an increase of 5% with a 28% increase in flow rate.

A final test of the method is to determine if it is independent of the amount of injectant W_0 ; that is, if the injectant size is changed, does the value of f remain unchanged? The experiment was repeated with all conditions duplicated except that the injectant volume was varied. These results are also shown in Table 3. Considering variations that accompany lower furnace temperatures, there appear to be only small differences in f , 6–9%, corresponding to 100% increases in the injectant volume.

Table 2. Values of f After Diffusion Eliminator Is Installed

Furnace Temp. K	f	
	Approx.	Exact
347	0.405	0.443
345	0.418	0.434
328	0.415	0.454
328	0.423	0.434
315	0.423	0.484
314	0.428	0.484

Table 3. Effect of Higher Purge Rates* and Different Injectant Sizes

Injection Size $\text{m}^3 \times 10^{10}$	f	
	Approx.	Exact
2	0.458	0.464
1	0.465	0.494
4	0.413	0.420

* $10.8 \times 10^{-3} \text{ m}^3/\text{s}$; Furnace temp., 323 K

Nevertheless, since injectant volumes may be very much lower for this type of calibration experiment than in actual reaction experiments, it is recommended that f values for different equipment be compared with a standard value of injection volume, say $2 \times 10^{-10} \text{ m}^3$.

Conclusions

The use of TGA data is often limited due to the difficulty in comparing one apparatus with another. This is a particular constraint when kinetic parameters are desired. The experimental techniques and modeling procedures presented here have been demonstrated to be useful indicators of TGA hydrodynamics. By proper selection of the amount and nature of adsorbent and adsorbate, we can predict the fraction f of pulsed injectant contacting a solid sample on the sample pan. This fraction increases when constrictors are placed in the TGA to eliminate back-diffusion; f also increases when the TGA is purged at higher rates with inert gas carrier. The fraction f has been shown to be relatively unaffected by changes in the size of injectant, within limits. Axial dispersion and other nonidealities in the micropulse can be neglected due to the small sample size of the micropulse, the injection technique, and the flow conditions inherently required for optimum microbalance performance in the TGA. The fraction f should be independent of temperature. However, in order to evaluate this parameter from adsorption/desorption data, the temperature should be kept as low as possible; on the other hand, the temperature controller works best at high temperatures. Temperatures ranging from 328 to 348 K are probably optimal.

Acknowledgment

The idea of this work grew out of a conversation with J. B. Cropley, Union Carbide Technical Center, South Charleston, WV. We acknowledge a useful conversation with L. Roberts. Acknowledgment is also made to National Science Foundation EPSCoR, Institutional Matching Project No. RII-8011453, for support of this work. We thank W. R. Grace for supplying the zeolite samples.

Notation

f = fraction of injectant contacting the sample
 G = amount of material present in gas phase above sample pan, kg
 k_a = pseudo-adsorption rate constant, s^{-1}
 k'_a = adsorption rate constant, $\text{kg}^{-1} \cdot \text{s}^{-1}$
 k_d = desorption rate constant, s^{-1}
 K = pseudo-adsorption equilibrium constant, $= k_a/k_d$
 t = time, s; $t = 0$ corresponds to adsorbent injection into the TGA
 t_m = time at which total mass of adsorbed injectant reaches maximum value, s
 t_o = time at which injectant is present above sample pan, $= V/v$, s

t_w = time at which mass of adsorbed injectant first reaches maximum mass of "irreversible" adsorbate, s
 T = temperature, K
 U = unit step function
 v = carrier gas volumetric flow rate, m³/s
 V = volume between injection point and sample pan, m³
 w = mass of adsorbate actually adsorbed at any time, kg
 w_a = maximum mass of "irreversible" adsorbate, kg
 w_i = mass of adsorbate "irreversibly" adsorbed at any time, kg
 w_m = maximum total mass of injectant actually adsorbed, kg
 w_o = maximum mass of adsorbate the adsorbent is capable of adsorbing, kg
 w_r = mass of adsorbate "reversibly" adsorbed at any time, kg
 W_o = total mass of adsorbate injected, kg
 $\delta(t - t_o)$ = Dirac delta function, = 0 everywhere except at $t = t_o$ and such that $\int \delta dt = 1$

Literature Cited

- Brown, N. L., J. C. Mullins, and S. S. Melsheimer, "A Nonlinear Equilibrium, Isothermal Fixed-Bed Adsorption Model Using Pulse Chromatographic Rate Parameters," *AIChE Symp. Ser.*, **74**(179), 9 (1978).
 Choudhary, V. R., and L. K. Doraiswamy, "Applications of Gas Chromatography in Catalysis," *Ind. Eng. Chem. Product Res. Dev.*, **10**, 219 (1971).
 Massoth, F. E., "Oxidation of Coked Silica-Alumina Catalyst," *Ind. Eng. Chem. Process Des. Dev.*, **6**, 200 (1967).
 Zweibel, I. and G. Yeo, "Fixed-Bed Adsorption with Concentrated Feeds," *AIChE Symp. Ser.* **74**(179), 19 (1978).

Manuscript received Jan. 5, 1987, and revision received May 5, 1987.